Linear Quadratic Integral Differential Game applied to the Real-time Control of a 3DoF Experimental setup of a Quadrotor

Hadi Nobahari
Department of Aerospace Engineering
Sharif University of Technology
Tehran, Iran
nobahari@sharif.edu

Ali BaniAsad
Department of Aerospace Engineering
Sharif University of Technology
Tehran, Iran
ali.baniasad@ae.sharif.edu

Alireza Sharifi
Department of Aerospace Engineering
Sharif University of Technology
Tehran, Iran
alireza_sharifi@ae.sharif.edu

***Abstract*—The accurate attitude control of a quadrotor is necessary, especially when facing disturbance. In this study, a linear quadratic with integral action based on the differential game theory is implemented on a three-degree-of-freedom experimental setup of a quadrotor. For this purpose, first, a continuous state-space model of the quadrotor is derived based on the linearization of the nonlinear equations of motion, and the parameters of the state-space model structure are identified with the experimental results. Then, the attitude control commands of the quadrotor are derived based on two players; one finds the best attitude control command, and the other creates the disturbance by minimizing a quadratic criterion, defined as the sum of outputs plus the weighted control effort. The performance of the proposed controller is evaluated in level flight and compared to the linear quadratic regulator controller. Results demonstrate that the proposed approach has an excellent performance in dissipating the disturbances created by the modeling error.**

***Index Terms*—Linear Quadratic Differential Game, Quadrotor, Real-time, 3DoF Experimental setup, Optimal Control, Robust Control**

I. Introduction

A quadrotor is a type of helicopter with four rotors that plays a significant role in today's society, including research, military, imaging, recreation, and agriculture. The performance of the quadrotor relies on the control system, including attitude, altitude, and position subsystems. In the attitude control of the quadrotor, it is necessary to maintain the attitude outputs, including roll, pitch, and yaw angles of the quadrotor, at the desired level using control commands such as the rotational speed of the rotors, mainly when the disturbances occur suddenly. Therefore, much research is being conducted on the automatic control of the attitudes' quadrotor in facing the disturbance. In [1], a Proportional Integral Derivative (PID) controller is used to control the attitude of the quadrotor. However, the control objectives have not been effectively achieved with this controllers category due to the nonlinearity of quadrotor dynamics, primarily when the disturbance occurs. The model-based approaches [2] for controller design are needed to solve these problems. These controllers work based on information from the dynamic attitude model of the quadrotor and the disturbance to produce the best control command. Various model-based controllers can be found within the literature, the most well-known of which are intelligent control, nonlinear control, robust control, and optimal control to reduce the disturbance effect in the attitude control and provide a faster control algorithm in facing the modeling error. In the intelligent controller category, artificial intelligence computing approaches like fuzzy logic [3], iterative learning [4], machine learning [5], reinforcement learning [6], and evolutionary computation [7] have been utilized to control the attitude of the quadrotor. Moreover, nonlinear control methods such as Sliding Mode Control (SMC) [8] and Feedback Linearization (FBL) [9] have been applied to control the roll, pitch, and yaw angles of the quadrotor. In the optimal controller category, a Linear Quadratic Regulator (LQR) [10] and Linear Quadratic Gaussian (LQG) [11] have been implemented on the wind turbine model based on the minimization of a quadratic criterion, including regulation performance and control effort to provide optimally controlled feedback gains. LQR-DG control approach [?] is a class of optimal and robust controller methods that controls the outputs of a system based on its linear model and minimization of a cost function. This approach has been utilized to stabilize and control various nonlinear and complex systems such as an ?? [?], a ?? [?], a ?? [?], and a ???. Moreover, in the LQR-DG control method, the control commands are analytically generated based on a pursuit-evasion of two players, one tracks the best attitude control command, and the other creates the disturbance. This is one of the distinctive features of the LQR-DG controller and an important difference from other optimal control methods. In this study, an LQIR method based on the differential game theory, called LQIR-DG, is proposed to generate the most efficient control command for an experimental setup of the quadrotor when facing the disturbance. Since the LQIR-DG is affected by an accurate model of the system, first, the dynamic of the three-degree-of-freedom setup of a quadrotor is modeled. Then, the linear state-space form of the wind turbine tower model is extracted using the linearization of the nonlinear equations of motion to utilize in the predictive control problem. Moreover, the

model's parameters are identified and verified against the experimental values. Next, the LQIR-DG technique is applied to the experimental setup of the quadrotor to reduce the effect of disturbance. The performance of the proposed controller is examined in the presence of the disturbance, including the modeling error. The results show the successful performance of the LQIR-DG scheme in reducing the disturbance. This paper is organized as follows: The problem architecture is defined in section 2. In section 3, the dynamics model for the experimental setup of the quadrotor is derived in detail. In section 4, The LQIR-DG architecture is denoted in section 5. Numerical results are provided in section 6. Finally, a conclusion is made in section 7.

II. Problem Statement

In this section, a nonlinear dynamic is presented for an experimental setup of a quadrotor, as shown in Fig.1. The quadrotor is free to rotate about its roll, pitch, and yaw axes. The Euler angle angles and angular velocities along three orthogonal axes are measured simultaneously using Attitude and Heading Reference Systems (AHRS). LQDG utilizes these noisy measurements for real-time control of the Euler angles. The block diagram of the control purpose is shown in Fig.2.

Fig. 1. 3DoF experimental setup of a quadrotor

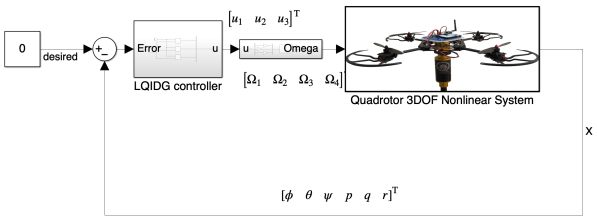

Fig. 2. block diagram of the control purpose

III. Modeling of an Experimental Setup of a Quadrotor

A. Configuration of the Quadrotor

The schematic of a quadrotor is given in Fig.3. Each rotor is considered a rigid disk is rotating about the axis Z_B in the body fixed frame with an angular velocity Ω_i. Rotors 1 and 3 rotate in the same direction, i.e., counterclockwise, while rotors 2 and 4 rotate in the opposite direction, i.e., clockwise, to cancel yawing moment of the quadrotor.

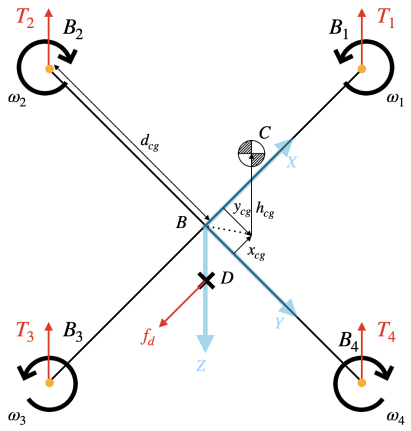

Fig. 3. Configuration of the quadrotor

B. Dynamic Model

The dynamic model of the quadrotor, obtained from the Newton-Euler method, is stated as follows [12], [13]:

$$\begin{aligned}
\dot{p} &= \frac{I_{yy}-I_{zz}}{I_{\text{xx}}}qr + q\frac{I_{\text{rotor}}}{I_{\text{xx}}}\Omega_r + \frac{u_{\text{roll}}}{I_{\text{xx}}} + \frac{d_{\text{roll}}}{I_{\text{xx}}} \\
\dot{q} &= \frac{I_{zz}-I_{zz}}{I_{yy}}rp + p\frac{I_{\text{rotor}}}{I_{\text{xx}}}\Omega_r + \frac{u_{\text{pitch}}}{I_{yy}} + \frac{d_{\text{pitch}}}{I_{yy}} \\
\dot{r} &= \frac{I_{\text{xx}}-I_{yy}}{I_{zz}}pq + \frac{u_{\text{yaw}}}{I_{zz}} + \frac{d_{\text{yaw}}}{I_{zz}}
\end{aligned} \tag{1}$$

where d_{roll}, d_{pitch}, and d_{yaw} are roll, pitch, and yaw moments, generated by the disturbance and (p, q, r) are the angular velocities, and (ϕ, θ, ψ) are roll, pitch, and yaw angles. The relation between Euler angles rates and the angular body rates are obtained as follows:

$$\begin{aligned}
\dot{\phi} &= p + q\sin(\phi)\cos(\theta) + r\cos(\phi)\tan(\theta) \\
\dot{\theta} &= q\cos(\phi) - r\sin(\phi) \\
\dot{\psi} &= (q\sin(phi) + r\cos(\phi))\sec(\theta)
\end{aligned} \tag{2}$$

where I_{xx}, I_{yy}, and I_{zz} are the principal moment of inertia and I_{rotor} is the inertia of a rotor about its axis. Moreover, Ω_r, called the overall residual propeller angular speed, is computed as:

$$\Omega_r = -\omega_1 + \omega_2 - \omega_3 + \omega_4 \tag{3}$$

The control inputs u_{roll}, u_{pitch}, and u_{yaw} are roll, pitch, and yaw moments, generated by the propellers, defined as:

$$\begin{aligned}
u_{\text{roll}} &= bd_{cg}(\Omega_2^2 - \Omega_4^2) \\
u_{\text{pitch}} &= bd_{cg}(\Omega_1^2 - \Omega_3^2) \\
u_{\text{yaw}} &= d(\Omega_1^2 - \Omega_2^2 + \Omega_3^2 - \Omega_4^2)
\end{aligned} \tag{4}$$

Also, b and d are thrust and drag coefficients, respectively, and d_{cg} is the horizontal distance of each rotor from the center

of gravity, as shown in Fig.3. Therefore, the angular velocity commands are obtained as:

$$\begin{aligned}
\Omega_{c,1}^2 &= \Omega_{\text{mean}}^2 + \frac{1}{2bd_{cg}}u_{\text{pitch}} + \frac{1}{4d}u_{\text{yaw}} \\
\Omega_{c,2}^2 &= \Omega_{\text{mean}}^2 + \frac{1}{2bd_{cg}}u_{\text{roll}} - \frac{1}{4d}u_{\text{yaw}} \\
\Omega_{c,3}^2 &= \Omega_{\text{mean}}^2 - \frac{1}{2bd_{cg}}u_{\text{pitch}} + \frac{1}{4d}u_{\text{yaw}} \\
\Omega_{c,4}^2 &= \Omega_{\text{mean}}^2 - \frac{1}{2bd_{cg}}u_{\text{roll}} - \frac{1}{4d}u_{\text{yaw}}
\end{aligned} \tag{5}$$

where Ω_{mean} is the average angular velocity of the rotors.

C. State-Space Form

Here, the state-space model of the experimental setup of the quadrotor is presented for the control purpose. by defining $x_1 = p$, $x_2 = q$, $x_3 = r$, $x_4 = \phi$, $x_5 = \theta$, and $x_6 = \psi$; the model of the experimental setup in state-space form are expressed as:

$$\begin{aligned}
\dot{x}_1 &= \frac{I_{yy} - I_{zz}}{I_{\text{xx}}}x_2x_3 + x_2\frac{I_{\text{rotor}}}{I_{\text{xx}}}\Omega_r + \frac{u_{\text{roll}}}{I_{\text{xx}}} + \frac{d_{\text{roll}}}{I_{\text{xx}}} \\
\dot{x}_2 &= \frac{I_{zz} - I_{zz}}{I_{yy}}x_1x_3 - x_1\frac{I_{\text{rotor}}}{I_{\text{xx}}}\Omega_r + \frac{u_{\text{pitch}}}{I_{yy}} + \frac{d_{\text{pitch}}}{I_{yy}} \\
\dot{x}_3 &= \frac{I_{\text{xx}} - I_{yy}}{I_{zz}}x_1x_2 + \frac{u_{\text{yaw}}}{I_{zz}} + \frac{d_{\text{yaw}}}{I_{zz}} \\
\dot{x}_4 &= x_1 + x_2\sin(x_4)\cos(x_5) + x_3\cos(x_4)\tan(x_5) \\
\dot{x}_5 &= x_2\cos(x_4) - x_3\sin(x_4) \\
\dot{x}_6 &= (x_2\sin(x_4) + x_3\cos(x_4))\sec(x_5)
\end{aligned} \tag{6}$$

The measurement model is written as:

$$\begin{aligned}
z &= \begin{bmatrix} p_m & q_m & r_m & \phi_m & \theta_m & \psi_m \end{bmatrix}^{\text{T}} \\
&= \begin{bmatrix} x_1 & x_2 & x_3 & x_4 & x_5 & x_6 \end{bmatrix}^{\text{T}}
\end{aligned} \tag{7}$$

D. Linear Model

The continuous-time linear model is utilized to drive the control commands on the quadrotor. The linear state-space model is denoted as:

$$\dot{\mathbf{x}}(t) = \mathbf{A}\mathbf{x}(t) + \mathbf{B}\mathbf{u}(t) + \mathbf{B_d}\mathbf{d}(t) \tag{8}$$

where d is the unknown input. $\mathbf{A}$, $\mathbf{B}$, and $\mathbf{B_d}$ are the system input and unknown input matrices, respectively. Moreover, the measurements equation is stated as:

$$\mathbf{z}(t) = \mathbf{C}\mathbf{x}(t) + \mathbf{D}\mathbf{u}(t) + \mathbf{D_d}\mathbf{d}(t) \tag{9}$$

where $\mathbf{C}$ is the output matrix. Also, $\mathbf{D}$ and $\mathbf{D_d}$ are the feedforward matrices due to known and unknown inputs, respectively. According to eq ? - ?, the linear dynamic model around the equilibrium points ($\mathbf{x}_e = 0$ and $\mathbf{u} = 0$) of the quadrotor setup is denoted as:

$$\begin{aligned}
\dot{\mathbf{x}} = \begin{bmatrix} \dot{\mathbf{x}}_{\text{roll}} \\ \dot{\mathbf{x}}_{\text{pitch}} \\ \dot{\mathbf{x}}_{\text{yaw}} \end{bmatrix} &= \begin{bmatrix} \mathbf{A}_{\text{roll}} & 0 & 0 \\ 0 & \mathbf{A}_{\text{pitch}} & 0 \\ 0 & 0 & \mathbf{A}_{\text{yaw}} \end{bmatrix} \begin{bmatrix} \mathbf{x}_{\text{roll}} \\ \mathbf{x}_{\text{pitch}} \\ \mathbf{x}_{\text{yaw}} \end{bmatrix} \\
&+ \begin{bmatrix} \mathbf{B}_{\text{roll}} & 0 & 0 \\ 0 & \mathbf{B}_{\text{pitch}} & 0 \\ 0 & 0 & \mathbf{B}_{\text{yaw}} \end{bmatrix} \begin{bmatrix} \mathbf{u}_{\text{roll}} \\ \mathbf{u}_{\text{pitch}} \\ \mathbf{u}_{\text{yaw}} \end{bmatrix} \\
&+ \begin{bmatrix} \mathbf{B}_{\text{roll}} & 0 & 0 \\ 0 & \mathbf{B}_{\text{pitch}} & 0 \\ 0 & 0 & \mathbf{B}_{\text{yaw}} \end{bmatrix} \begin{bmatrix} \mathbf{d}_{\text{roll}} \\ \mathbf{d}_{\text{pitch}} \\ \mathbf{d}_{\text{yaw}} \end{bmatrix}
\end{aligned} \tag{10}$$

where $x_{\text{roll}} = \begin{bmatrix} p & \phi \end{bmatrix}^{\text{T}}$, $x_{\text{pitch}} = \begin{bmatrix} q & \theta \end{bmatrix}^{\text{T}}$, and $x_{\text{yaw}} = \begin{bmatrix} r & \psi \end{bmatrix}^{\text{T}}$. Also $d = \begin{bmatrix} x \end{bmatrix}^{\text{T}}$, is the ..... . Moreover, the state and input matrices are derived as:

$$\mathbf{A}_{\text{roll}} = \begin{bmatrix} 0 & 1 \\ 0 & 0 \end{bmatrix};\ \mathbf{A}_{\text{pitch}} = \begin{bmatrix} 0 & 1 \\ 0 & 0 \end{bmatrix};\ \mathbf{A}_{\text{yaw}} = \begin{bmatrix} 0 & 1 \\ 0 & 0 \end{bmatrix} \tag{11}$$

$$\mathbf{B}_{\text{roll}} = \begin{bmatrix} 0 \\ \frac{1}{I_{\text{xx}}} \end{bmatrix};\ \mathbf{B}_{\text{pitch}} = \begin{bmatrix} 0 \\ \frac{1}{I_{yy}} \end{bmatrix};\ \mathbf{B}_{\text{yaw}} = \begin{bmatrix} 0 \\ \frac{1}{I_{zz}} \end{bmatrix} \tag{12}$$

E. Parameter Estimation

This section modifies the quadrotor stand parameters using the Simulink environment's simulation of different quadrotor channels and the stand's output data. The quadrotor stand parameters have been modified using the Parameter Estimator toolbox available in the Simulink environment. In order to perform the test, the quadrotor stand was released from various initial conditions and inputs, and data was collected using the output from the sensor. Then, Parameter Estimator takes the model and the recorded data of the sensor (stand states). Here is a comparison between the states of the quadrotor in simulation and reality after modifying various parameters.

TABLE I
PARAMETER ESTIMATION RESULTS

Parameter	***Value***	***Units***
I_{xx}	0.02839	$kg.m^2$
I_{yy}	0.03066	$kg.m^2$
I_{zz}	0.0439	$kg.m^2$
I_{rotor}	4.4398×10^{-5}	$kg.m^2$

IV. DIFFERENTIAL GAME

Differential games are a series of problems that arise while examining and simulating dynamic systems in game theory. Differential equations simulate how a state variable or set of state variables changes over time.

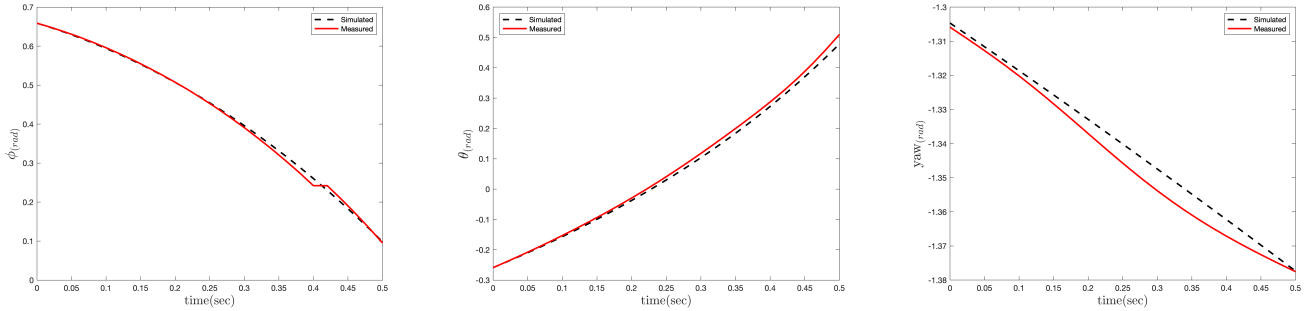

(a) Roll Channel (b) Pitch Channel (c) Yaw Channel

Fig. 4. Comparison of quadrotor states in simulation and reality.

A. Differential Game Usage in a Quadrotor Control Loop

This paper describes the state of two players in different loop control of a quadrotor. Three groups of players are identified: two players for roll loop control, two players for pitch loop control, and two players for yaw loop control. The space state of roll, pitch, and yaw are defined below.

$$\begin{aligned}\dot{\mathbf{x_i}}(t) &= \mathbf{A_i}\mathbf{x_i}(t) + \mathbf{B_i}\mathbf{u_i}(t) + \mathbf{B_{i_d}}\mathbf{u_{i_d}}(t)\\ \mathbf{y_i}(t) &= \mathbf{C_i}\mathbf{x_i}(t) + \mathbf{D_i}\mathbf{u_i}(t) + \mathbf{D_{i_d}}\mathbf{u_{i_d}}(t)\\ i &= 1,2,3\end{aligned} \tag{13}$$

Where $\mathbf{x}$ is the vector of the state variables, $\dot{\mathbf{x}}$ is the time derivative of the state vector, $\mathbf{u}$ is the controller input vector, $\mathbf{u_d}$ is the disturbance input vector, $\mathbf{y}$ is the output vector, $\mathbf{A}$ is the state matrix, $\mathbf{B}$ is the controller input matrix, $\mathbf{B_d}$ is the disturbance input matrix, $\mathbf{C}$ is the output matrix, $\mathbf{D}$ is controller the output matrix and $\mathbf{D_d}$ is disturbance the output matrix. Equation (13) demonstrates how both participants have an impact on the quadrotor's dynamics. The second player may progress toward the goal as a result of the first player's exertion, or vice versa. This paper considers the case that players do not cooperate in order to realize their goals. In this case, every player knows at time $t \in [0, T]$ just the initial state $\mathbf{x_0}$ and the model structure. For the game between two players in each loop control, the set of Nash equilibria is used. Formal Nash equilibrium is defined as follows. An admissible set of actions $(\boldsymbol{u_1}^*, \boldsymbol{u_{i_d}}^*)$ is a Nash equilibrium for the game between two player in each loop control; if for all admissible $(\boldsymbol{u_i}, \boldsymbol{u_{i_d}})$, the following inequalities hold:

$$J_1(\mathbf{u_i}^*, \mathbf{u_{i_d}}^*) \leq J_1(\mathbf{u_1}, \mathbf{u_{i_d}}^*)\ ,\ J_2(\mathbf{u_i}^*, \mathbf{u_{i_d}}^*) \leq J_2(\mathbf{u_i}^*, \mathbf{u_{i_d}}) \tag{14}$$

B. LQDG controller

For the each control loop described in equation (13), LQDG optimum control effort calculates from equation (15).

$$\mathbf{u_i}(t) = -\mathbf{R_i}^{-1}\mathbf{B_i}^{\mathrm{T}}\mathbf{P_i}(t)\mathbf{x}(t) = -\mathbf{K_i}(t)\mathbf{x}(t), \quad i = 1,2,3 \tag{15}$$

In equation (15), $\mathbf{K_i}$ is the optimal feedback gain. Assuming that the other players will make their worst move, this gain is calculated to minimize the quadratic cost function equation (16) of controller player for each control loop of quadrotor.

$$J_i(\mathbf{u_i}, \mathbf{u_{i_d}}) = \int_0^T \Big(\mathbf{x_i}^{\mathrm{T}}(t)\mathbf{Q_i}\mathbf{x_i}(t) + \mathbf{u_i}^{\mathrm{T}}(t)\mathbf{R_i}\mathbf{u_i}(t) + \mathbf{u_{i_d}}^{\mathrm{T}}(t)\mathbf{R_{i_d}}\mathbf{u_{i_d}}(t) \Big) \mathrm{d}t, \quad i = 1,2,3 \tag{16}$$

Here the matrices $\mathbf{Q_i}$ and $\mathbf{R_i}$ are assumed to be symmetric and $\mathbf{R_i}$ positive definite. $\mathbf{P_i}$ is found by solving the continuous time couple Riccati differential equation:

$$\begin{aligned}\dot{\mathbf{P}}_{\boldsymbol{i}}(t) &= -\mathbf{A_i}^{\mathrm{T}}\mathbf{P_i}(t) - \mathbf{P_i}(t)\mathbf{A_i} - \mathbf{Q_i} + \mathbf{P_i}(t)\mathbf{S_i}(t)\mathbf{P_i}(t) + \\ &\quad \mathbf{P_i}(t)\mathbf{S_{i_d}}(t)\mathbf{P_{i_d}}(t)\\ \dot{\mathbf{P}}_{\boldsymbol{i_d}}(t) &= -\mathbf{A_i}^{\mathrm{T}}\mathbf{P_{i_d}}(t) - \mathbf{P_{i_d}}(t)\mathbf{A_i} - \mathbf{Q_{i_d}} + \\ &\quad \mathbf{P_{i_d}}(t)\mathbf{S_{i_d}}(t)\mathbf{P_{i_d}}(t) + \mathbf{P_{i_d}}(t)\mathbf{S_i}(t)\mathbf{P_i}(t)\end{aligned} \tag{17}$$

Using the shorthand notation $\boldsymbol{S_i} := \boldsymbol{B_i}\boldsymbol{R_i}^{-1}\boldsymbol{B_i}^{\mathrm{T}}$.

C. LQIDG controller

The absence of an integrator in the LQDG controller may result in steady-state errors due to disturbances or modeling errors. The LQIDG controller is based on the LQDG controller to eliminate this error.

The LQIDG controller adds the integral of the difference between the system output and the desired value to the state vector. Therefore, The augmented space states of a continuous linear system are shown below.

$$\mathbf{x_a} = \begin{bmatrix} \mathbf{x_d} - \mathbf{x} \\ \int (\mathbf{y_d} - \mathbf{y}) \end{bmatrix} \tag{18}$$

Where $\mathbf{x_a}$ is the vector of augmented state variables, $\mathbf{x_d}$ is the vector of the desired state variables, and $\mathbf{y_d}$ is the desired output vector. As a result, the state vector and the output vector are equal.

$$\mathbf{y} = \mathbf{x} \tag{19}$$

The following represents the system dynamics in the augmented state space.

$$\dot{\mathbf{x}}_{\boldsymbol{a}}(t) = \mathbf{A_a}\mathbf{x_a}(t) + \mathbf{B_{a_1}}\mathbf{u_{a_1}}(t) + \mathbf{B_{a_2}}\mathbf{u_{a_2}}(t) \tag{20}$$

Where matrices $\mathbf{A_a}$ and $\mathbf{B_a}$ are defined as follows:

$$\mathbf{A_a} = \begin{bmatrix} \mathbf{A} & 0 \\ \mathbf{C} & 0 \end{bmatrix}, \quad \mathbf{B_a} = \begin{bmatrix} \mathbf{B} \\ 0 \end{bmatrix} \tag{21}$$

By introducing a new space state for the system, the remaining design phases of the LQIDG controller are comparable to those of the LQDG controller. LQIDG optimum control effort calculates from equation (22).

$$\begin{aligned} \mathbf{u_i}(t) &= -\mathbf{R_{ii}}^{-1}\mathbf{B_{a_i}}^{\mathrm{T}}\mathbf{P_{a_i}}(t)\mathbf{x_a}(t) \\ \mathbf{u_i}(t) &= -\mathbf{K_{a_i}}(t)\mathbf{x_a}(t), \ i = 1, 2, 3 \end{aligned} \tag{22}$$

In equation (22), $\mathbf{K_{a_i}}$ is the optimal feedback gain. Assuming that the other players will make their worst move, this gain is calculated to minimize the quadratic cost function, equation (23), of player number i.

$$J_i(\mathbf{u_i}, \mathbf{u_{i_d}}) = \int_0^T \Big(\mathbf{x_a}^{\mathrm{T}}(t)\mathbf{Q_i}\mathbf{x_a}(t) + \mathbf{u_i}^{\mathrm{T}}(t)\mathbf{R_i}\mathbf{u_i}(t) + \mathbf{u_{i_d}}^{\mathrm{T}}(t)\mathbf{R_{i_d}}\mathbf{u_{i_d}}(t) \Big) \mathrm{d}t \tag{23}$$

$\dot{\mathbf{P}}_{\boldsymbol{a_i}}$ is found by solving the continuous time couple Riccati differential equation:

$$\begin{aligned} \dot{\mathbf{P}}_{\boldsymbol{a_i}}(t) &= -\mathbf{A_a}^{\mathrm{T}}\mathbf{P_{a_i}}(t) - \mathbf{P_{a_i}}(t)\mathbf{A_a} - \mathbf{Q_i} + \\ &\quad \mathbf{P_{a_i}}(t)\mathbf{S_{a_i}}(t)\mathbf{P_{a_i}}(t) + \mathbf{P_{a_i}}(t)\mathbf{S_{a_{i_d}}}(t)\mathbf{P_{a_{i_d}}}(t) \\ \dot{\mathbf{P}}_{\boldsymbol{a_{i_d}}}(t) &= -\mathbf{A_a}^{\mathrm{T}}\mathbf{P_{a_{i_d}}}(t) - \mathbf{P_{a_{i_d}}}(t)\mathbf{A_a} - \mathbf{Q_{i_d}} + \\ &\quad \mathbf{P_{a_{i_d}}}(t)\mathbf{S_{a_{i_d}}}(t)\mathbf{P_{a_{i_d}}}(t) + \mathbf{P_{a_{i_d}}}(t)\mathbf{S_{a_i}}(t)\mathbf{P_{a_i}}(t) \end{aligned} \tag{24}$$

Using the shorthand notation $\boldsymbol{S_{a_i}} := \boldsymbol{B_{a_i}}\boldsymbol{R_i}^{-1}\boldsymbol{B_{a_i}}^{\mathrm{T}}$.

V. Simulation

In this section, the quadrotor roll loop control is simulated in the presence of LQR, LQDG, and LQIDG controllers. Then, the simulation of two and three degrees of freedom was done in the presence of the LQIDG controller.

A. Roll Loop Control

LQR weighting matrices are optimized using the TCACS optimization method in the simulation. ITSE is considered for the TCACS input cost function. Here are the weighting matrices for the optimized output.

$$\mathbf{Q}_{\mathrm{LQR}} = \begin{bmatrix} 0.5215 & 0 \\ 0 & 0.0745 \end{bmatrix}, \quad R_{\mathrm{LQR}} = 0.0001 \tag{25}$$

The weighting matrices used in the LQDG portion are chosen like that of the LOR.

$$\mathbf{Q}_{\mathrm{LQDG}} = \begin{bmatrix} 100 & 0 \\ 0 & 0.078 \end{bmatrix}, \quad R_{\mathrm{LQDG}} = 1, \quad R_{d_{\mathrm{LQDG}}} = 99.96 \tag{26}$$

$$\mathbf{K_1} = \begin{bmatrix} 39.1188 & 8.8510 \end{bmatrix} \tag{27}$$

LQIDG weighting matrices are chosen like the method used in the LQR and LQDG sections.

$$\mathbf{Q}_{\mathrm{LQIDG}} = \begin{bmatrix} 0.1707 & 0 & 0 & 0 \\ 0 & 0.12 & 0 & 0 \\ 0 & 0 & 837.8606 & 0 \\ 0 & 0 & 0 & 756.1341 \end{bmatrix} \tag{28}$$

$$R_{\mathrm{LQIDG}} = 1, \quad R_{d_{\mathrm{LQIDG}}} = 7.7422$$

$$\mathbf{K_{a_1}} = \begin{bmatrix} 28.1410 & 8.4017 & 27.2223 & 11.6894 \end{bmatrix} \tag{29}$$

B. Roll-Pitch Loop Control

$$\begin{aligned} \mathbf{Q}_{\mathrm{LQIDG_{roll}}} &= \begin{bmatrix} 585.9 & 0 & 0 & 0 \\ 0 & 31.1 & 0 & 0 \\ 0 & 0 & 83.8 & 0 \\ 0 & 0 & 0 & 0 \end{bmatrix} \\ \mathbf{Q}_{\mathrm{LQIDG_{pitch}}} &= \begin{bmatrix} 546.5 & 0 & 0 & 0 \\ 0 & 311.4 & 0 & 0 \\ 0 & 0 & 2.22 & 0 \\ 0 & 0 & 0 & 0 \end{bmatrix} \end{aligned} \tag{30}$$

$$R_{\mathrm{LQIDG}} = 1, \quad R_{d_{\mathrm{LQIDG}}} = 7.7422$$

C. Roll-Pitch-Yaw Loop Control

$$\begin{aligned} \mathbf{Q}_{\mathrm{LQIDG_{roll}}} &= \begin{bmatrix} 631.85 & 0 & 0 & 0 \\ 0 & 214.28 & 0 & 0 \\ 0 & 0 & 7.91 & 0 \\ 0 & 0 & 0 & 0.01 \end{bmatrix} \\ \mathbf{Q}_{\mathrm{LQIDG_{pitch}}} &= \begin{bmatrix} 0.01 & 0 & 0 & 0 \\ 0 & 873.93 & 0 & 0 \\ 0 & 0 & 9853.09 & 0 \\ 0 & 0 & 0 & 0.12 \end{bmatrix} \\ \mathbf{Q}_{\mathrm{LQIDG_{yaw}}} &= \begin{bmatrix} 0.03 & 0 & 0 & 0 \\ 0 & 0.17 & 0 & 0 \\ 0 & 0 & 1.81 & 0 \\ 0 & 0 & 0 & 0.45 \end{bmatrix} \times 10^{-4} \end{aligned} \tag{31}$$

$$R_{\mathrm{LQIDG}} = 1, \quad R_{d_{\mathrm{LQIDG}}} = 1.2577$$

VI. Result and Discussion

Here, the results of the LQIR-DG controller method are devoted to the control loops of the roll, pitch, and yaw of the experimental setup of the quadrotor. First, the controller parameters are tuned using the results of numerical simulations. Moreover, the performance of the LQIR-DG controller is compared to an LQR control strategy.

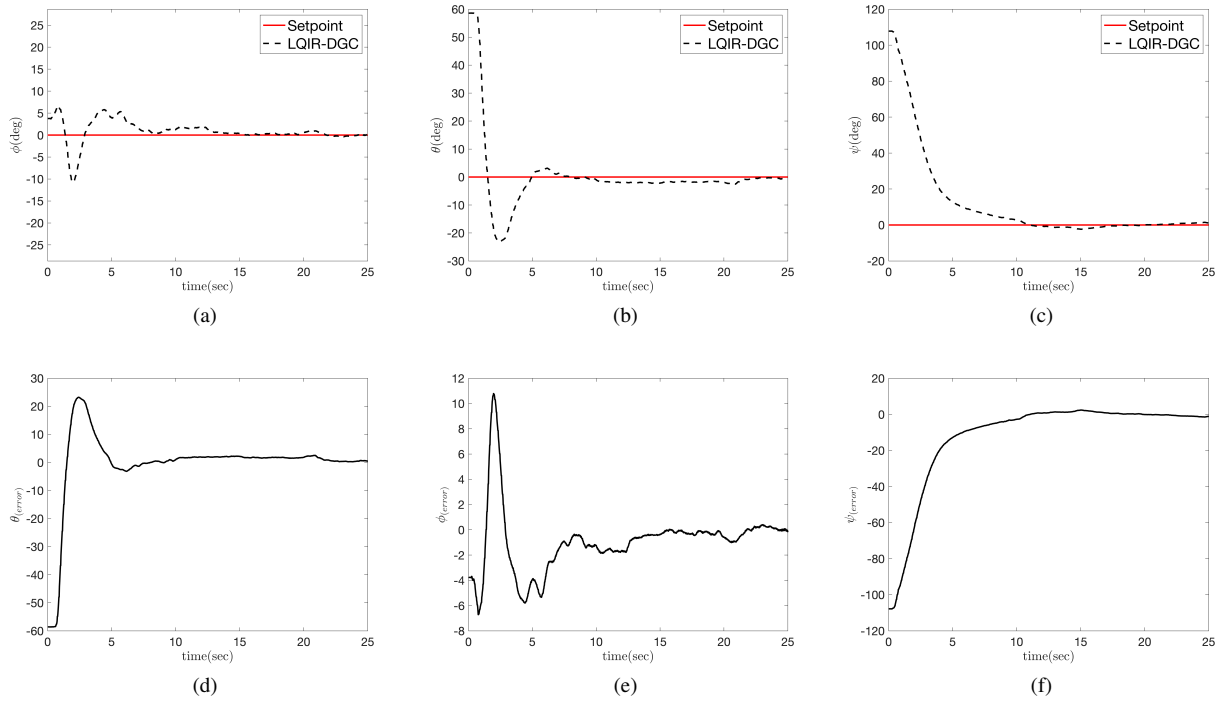

Fig. 5. Performance of the LQIR-DG controller (a) Desired and actual roll angle (b) Desired and actual pitch angle (c) Desired and actual yaw angle.

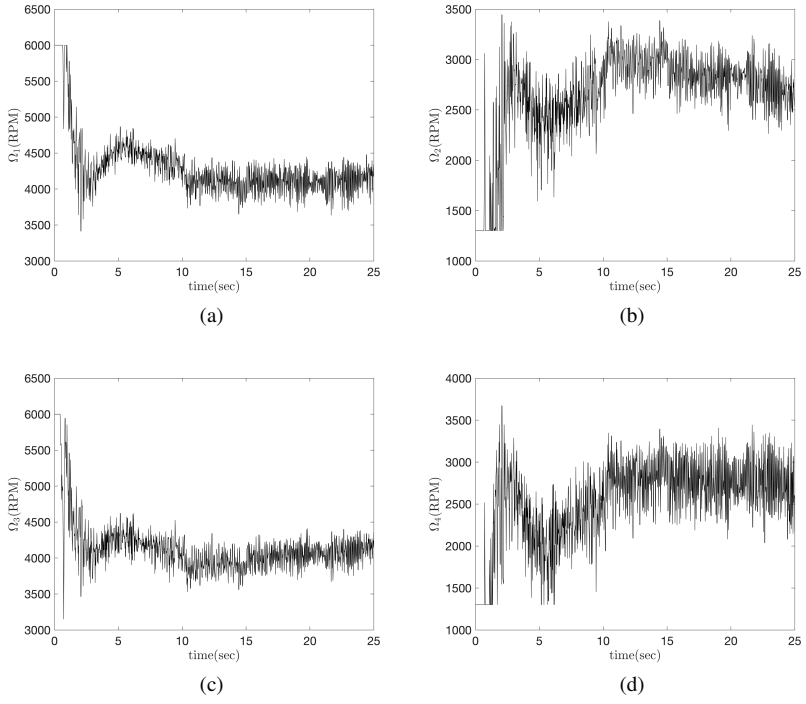

Fig. 6. implementation result omega

A. *Performance of the LQIR-DG Controller*

The performance of the LQIR-DG controller is evaluated in Figure 8. The desired and actual outputs, including the roll, pitch, and yaw angles, are compared in Figures 8 (a) and (b). The desired scenario of the simulator is considered a level flight. These figures show that the attitude outputs of the quadrotor converge to the desired values in less than three seconds. Moreover, Figures 8 (c) and (d) show the angular

velocity command of the quadrotor, respectively. These results illustrate that the LQIR-DG approach appropriately controls the attitude of the experimental setup of the quadrotor.

TABLE II
LQIR-DG CONTROL PARAMETER

Control Loop	q_1	q_2	q_3	q_4
Roll	631.85	214.28	7.91	0.01
Pitch	0.01	873.93	9853.09	0.12
Yaw	3×10^{-6}	1.7×10^{-5}	1.81×10^{-4}	4.5×10^{-5}

TABLE III
LQIR-DG CONTROL PARAMETER

Control Loop	q_1	q_2	q_3	q_4
Roll	631.85	214.28	7.91	0.01
Pitch	0.01	873.93	9853.09	0.12
Yaw	$3e-6$	$1.7e-5$	$1.81e-4$	$4.5e-5$

B. Comparison with Well-known Control Strategies

Here, the LQIR-DG controller performance is compared with famous control strategies such as the LQR Figure 10. Figure 10 (a) compares the quadrotor's desired and actual pitch angle in the presence of these controllers. These results indicate that the LQIR-DG controller can provide high tracking performance, such as good transient response and high rapid convergence relative to other controllers for pitch angle control of the experimental setup of the quadrotor.

VII. CONCLUSION

In this study, a linear quadratic with integral action based on the differential game theory, called LQIR-DG, was implemented for level attitude control in an experimental setup of a quadrotor. To implement the proposed controller structure, first, an accurate dynamic model of the quadrotor was linearized in the state-space form, and then the model parameters were estimated. Next, two players were considered for each of the quadrotor's roll, pitch, and yaw channels. The first player found the best control command for each channel of the setup of a quadrotor based on the minimization of a quadratic criterion; when the second player produced the disturbances. Finally, the performance of the proposed controller was evaluated in level flight and compared to the LQR controller. The implementation results verify the successful performance of the LQIR-DG method in the level of attitude control of the experimental setup of the quadrotor.

REFERENCES

[1] H. Bolandi, M. Rezaei, R. Mohsenipour, H. Nemati and S. Smailzadeh, "Attitude Control of a Quadrotor with Optimized PID Controller," Intelligent Control and Automation, Vol. 4 No. 3, 2013, pp. 335-342. doi: 10.4236/ica.2013.43039.

[2] Bouzid, Y., Zareb, M., Siguerdidjane, H. et al. Boosting a Reference Model-Based Controller Using Active Disturbance Rejection Principle for 3D Trajectory Tracking of Quadrotors: Experimental Validation. J Intell Robot Syst 100, 597–614 (2020). https://doi.org/10.1007/s10846-020-01182-4

[3] K. Liu, R. Wang, S. Dong and X. Wang, "Adaptive Fuzzy Finite-time Attitude Controller Design for Quadrotor UAV with External Disturbances and Uncertain Dynamics," 2022 8th International Conference on Control, Automation and Robotics (ICCAR), 2022, pp. 363-368, doi: 10.1109/ICCAR55106.2022.9782598.

[4] L. V. Nguyen, M. D. Phung, and Q. P. Ha, "Iterative Learning Sliding Mode Control for UAV Trajectory Tracking," Electronics, vol. 10, no. 20, 2021, doi: 10.3390/electronics10202474.

[5] C. Nicol, C. J. B. Macnab and A. Ramirez-Serrano, "Robust neural network control of a quadrotor helicopter," 2008 Canadian Conference on Electrical and Computer Engineering, 2008, pp. 001233-001238, doi: 10.1109/CCECE.2008.4564736.

[6] C.-H. Pi, W.-Y. Ye, and S. Cheng, "Robust Quadrotor Control through Reinforcement Learning with Disturbance Compensation," Applied Sciences, vol. 11, no. 7, 2021, doi: 10.3390/app11073257.

[7] P. Ghiglino, J. L. Forshaw, and V. J. Lappas, "Online PID Self-Tuning using an Evolutionary Swarm Algorithm with Experimental Quadrotor Flight Results," in AIAA Guidance, Navigation, and Control (GNC) Conference, doi: 10.2514/6.2013-5098.

[8] H. Wang and M. Chen, "Sliding mode attitude control for a quadrotor micro unmanned aircraft vehicle using disturbance observer," Proceedings of 2014 IEEE Chinese Guidance, Navigation and Control Conference, 2014, pp. 568-573, doi: 10.1109/CGNCC.2014.7007285.

[9] A. Aboudonia, A. El-Badawy, and R. Rashad, "Disturbance observer-based feedback linearization control of an unmanned quadrotor helicopter," Proceedings of the Institution of Mechanical Engineers, Part I: Journal of Systems and Control Engineering, vol. 230, no. 9, pp. 877–891, 2016, doi: 10.1177/0959651816656951.

[10] Z. Shulong, A. Honglei, Z. Daibing and S. Lincheng, "A new feedback linearization LQR control for attitude of quadrotor," 2014 13th International Conference on Control Automation Robotics & Vision (ICARCV), 2014, pp. 1593-1597, doi: 10.1109/ICARCV.2014.7064553.

[11] E. Barzanooni, K. Salahshoor and A. Khaki-Sedigh, "Attitude flight control system design of UAV using LQG multivariable control with noise and disturbance," 2015 3rd RSI International Conference on Robotics and Mechatronics (ICROM), 2015, pp. 188-193, doi: 10.1109/ICRoM.2015.7367782.

[12] Bouabdallah, S., 2007. Design and Control of Quadrotors with Application to Autonomous Flying (Ph.D. thesis), University of Pennsylvania, Philadelphia.

[13] S. Bouabdallah and R. Siegwart, "Full control of a quadrotor," 2007 IEEE/RSJ International Conference on Intelligent Robots and Systems, 2007, pp. 153-158, doi: 10.1109/IROS.2007.4399042.